

# DESIGN OF 9/6 MeV S-BAND ELECTRON LINAC STRUCTURE WITH 1.5 BUNCHING CELLS

Youngwoo Joo<sup>1,2\*</sup>, Yujong Kim<sup>1†</sup>, Pikad Buaphad<sup>1,2</sup>, Sungsu Cha<sup>1</sup>, and Hyeri Lee<sup>1,2</sup>

<sup>1</sup>Future Accelerator R&D Team, Nuclear Data Center, KAERI, Daejeon 34057, Korea

<sup>2</sup>Dept. of Accelerator and Nuclear Fusion Physical Engineering, UST Daejeon 34113, Korea

## Abstract

The Korea Atomic Energy Research Institute (KAERI) has been developing several 9/6 MeV dual energy S-band RF electron linear accelerators (linacs) for non-destructive testing such as container inspection system. Until now, the bunching cell of the linac has a full-cell geometry. However, to maximize the acceleration of electrons after emission from the electron gun, the geometry of the first bunching cell is modified from a full-cell to a half-cell. The optimization of Q-factor and flatness of electric field along the linac structure can be obtained by adjusting diameters of bunching and power coupling cells. By adjusting gap of the first side-coupling cell, we can optimize the field ratio between the bunching cells and normal accelerating cells. In this paper, we describe design concepts of a 9/6 MeV linac with 1.5 bunching cells as well as optimization of RF parameters such as the quality factor, resonance frequency, and electric field distribution.

## INTRODUCTION

Electron accelerators have been widely used for industrial/medical applications such as radiation processing and non-destructive testing (NDT). NDT is a popular analysis technique used in science and industrial technology to evaluate the properties of a material or an object without any big damage. Recently, to perform inspection of large size objects such as containers, demands of high energy electron linear accelerators for industrial cargo inspection system have been rapidly increasing [1]. The cargo inspection system consists of an electron linear accelerator, a target to generate bremsstrahlung X-rays, and a detector. X-rays can be used to make clean images of hidden objects in the container by using the detector. After consideration of a high neutron generation at a beam energy higher than 10 MeV and penetration capability of X-rays over 40 cm thick iron plates [2], 9 MeV was selected as the maximum beam energy of the linac for the container inspection system. In addition, we selected 9/6 MeV pulse-by-pulse dual energy to distinguish between organic matters and inorganic ones in the container [3]. To build an electron linac for the container inspection system, we designed an S-band linac structure by performing numerous CST simulations. The accelerating linac structure for the container inspection system consists of bunching cells, accelerating cells, side-coupling cells, and an RF power coupling cell.

Originally, in 2013, KAERI successfully fabricated an electron linac structure with a full-cell geometry for the first bunching cell [4]. However, with the full-cell geometry, the accelerating field is not maximum at the entrance of the bunching cell. Therefore, beam acceleration is not effective, and the space charge force is strong due to the lower energy at the entrance region [5]. In this case, there is a limitation in obtaining high beam current at the end of the linac structure. To solve that problem, we modified the full-cell geometry into a half-cell, which can supply the maximum accelerating field at the entrance of the bunching cell [6]. In this paper, we describe design concepts and optimizations of a new 9/6 MeV electron linac structure with 1.5 bunching cells for the container inspection system.

## DESIGN CONCEPT

The structure chain has a basic unit, which consists of two plates as shown in Fig. 1. According to the different combinations of those two plates, the basic unit is divided into two types: the first type (HA-SC-HA) with a half accelerating cell (HA), a side-coupling cell (SC), and a half accelerating cell (HA), and the second type (HS-AC-HS) with a half side-coupling cell (HS), an accelerating cell (AC), and a half side-coupling cell (HS). Finally, each cell is tuned again to allow the  $\pi/2$  mode frequency of the structure to be close to the target frequency (= 2856 MHz) [7]. The design goal is making a shunt impedance of 70 M $\Omega$ /m, a beta coupling of 2.84, and a beam current of 50 mA to get a beam energy of 9 MeV with 3 MW as shown in Fig. 2 and to achieve uniform electric field distribution at 2856 MHz [2, 8, 9].

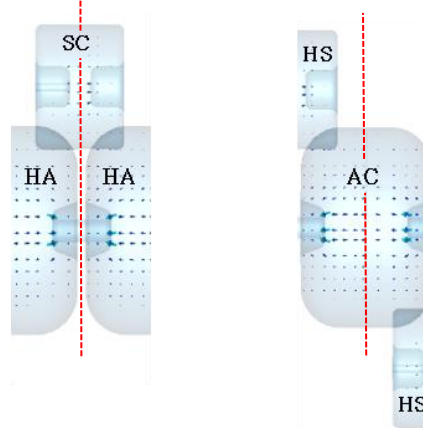


Figure 1: HA-SC-HA and HS-AC-HS types.

\* ywjoo@kaeri.re.kr

† yjkim@kaeri.re.kr

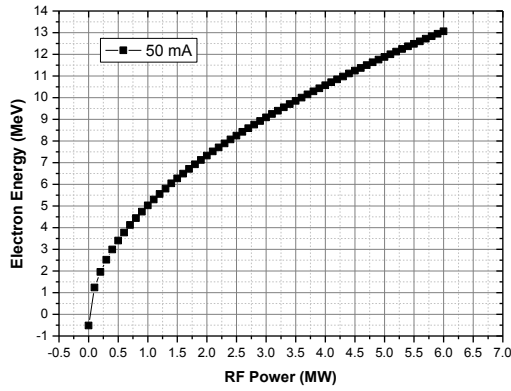


Figure 2: RF power requirement for 9 MeV.

### DESIGN OF BUNCHING CELLS AND POWER COUPLING CELL

The accelerating structure consists of 1.5 bunching cells, a power coupling cell, and eight normal accelerating cells as shown in Figs. 3, 4, and 5. The bunching cells are accelerating cells with its relative velocity less than 1 for bunching. According to electron beam energy, their cell lengths are shorter than those of normal accelerating cells. The maximum peak beam current or shortest bunch length can be obtained by optimizing geometry of those bunching cells.

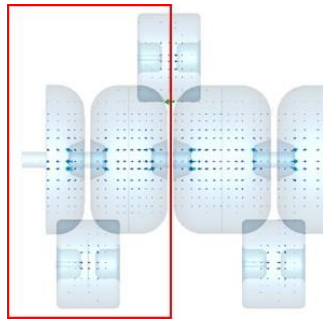


Figure 3: 1.5 Bunching cells.

Since the electric field is maximum at the middle position of a cell, we can maximize acceleration at the entrance of the first bunching cell by selecting a half-cell geometry for the cell. A power coupler is used to transfer RF power from an RF source to the structure through the coupling cell. The power coupler consists of a power coupling cell and a tapered rectangular waveguide section as shown in Fig. 4 [10]. According to the requirement of RF power transmission, we adjust geometric parameters of waveguide and tapered waveguide to minimize the reflected power. The reflected power can be minimized by optimizing coupling coefficient. The optimized coupling coefficient for 9 MeV can be given by

$$\beta = 1 + \frac{P_b}{P_d} = 1 + \frac{I_p R_{sh} l}{V_{acc}} = 1 + \frac{1.2 \text{ MW}}{0.66 \text{ MW}} = 2.84, \quad (1)$$

where  $P_b$  is the beam power,  $P_d$  is the power dissipated in cavity wall,  $I_p$  is the peak beam current at the target,  $R_{sh}$

is the shunt impedance per unit length,  $l$  is the linac length, and  $V_{acc}$  is the electron energy/(electron charge  $e = -1.6 \times 10^{-19} \text{ C}$ ). Similarly, for 6 MeV, the optimized coupling coefficient is 3.27 with 1.5 MW. Therefore for the 9/6 MeV dual energy operation, an average coupling coefficient of 3.06 is chosen to obtain the minimum reflected power from the power coupler at the resonance frequency of 2856 MHz for the  $\pi/2$  mode of the structure.

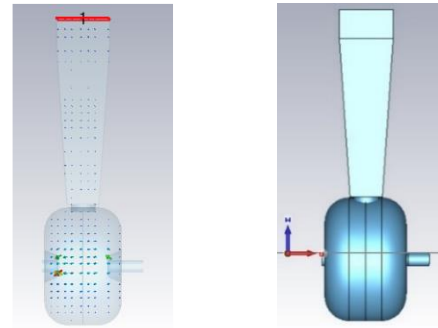


Figure 4: Power coupling cell.

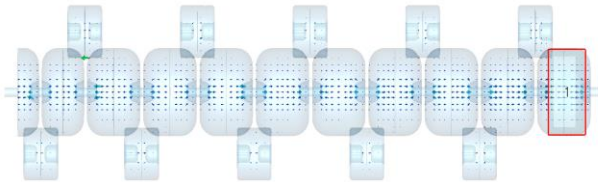


Figure 5: Electric field distribution in the linac.

### OPTIMIZATION OF ELECTRIC FIELD DISTRIBUTION

From geometry optimizations of 1.5 bunching cells, eight accelerating cells and a power coupling cell, we can obtain CST simulations of individual components. By tuning the resonance frequencies of 1.5 bunching cells and nine accelerating cells including a coupling cell, we combine whole linac structure to obtain a reasonably uniform electric field distribution along the structure. The best result of the Q-factor and uniform electric field distribution can be obtained when the diameter of the bunching cell is 75.8 mm, and that of the power coupling cell is 75.2 mm as shown in Figs. 5 and 6. Since acceleration efficiency of electron beams is directly related to uniformity and magnitude of electric field, they are the most important things, which we have to take care of during the structure tuning [9, 11, 12]. The ratio of electric field between the first bunching cell and normal accelerating cells can be changed by adjusting the gap of the first side-coupling cell. Figure 6 shows the electric field distribution when Gap Lengths of Side-coupling cell (GLS) has three different ratios of 0.8, 0.9, and 1.0. Here, GLS ratio of 0.9 means that the gap length in the first side-coupling cell is reduced by 10% from the nominal one. Those results demonstrate that the gap of the side-coupling cell is also an important tuning parameter because it is related to the electron capturing coefficient, current, and energy. Table 1 shows that a higher energy and a higher current can be obtained when

GLS is 0.8 or 0.9 instead of 1.0. Electron energy at the gun exit is 20 keV, and the final optimized electron beam current and energy are summarized in Table 1. Figure 7 shows the CST Particle In Cell (PIC) simulation result when GLS is 0.8. In the near future, we will improve the PIC simulation further [6].

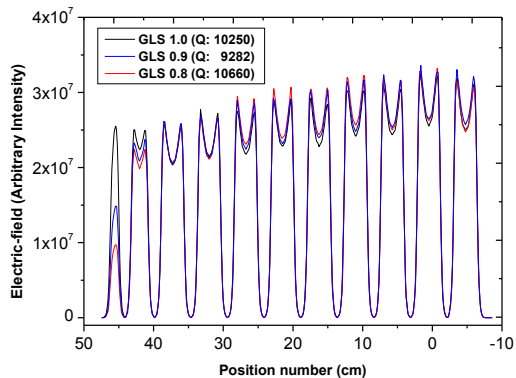


Figure 6: E-field distribution for three different GLSs.

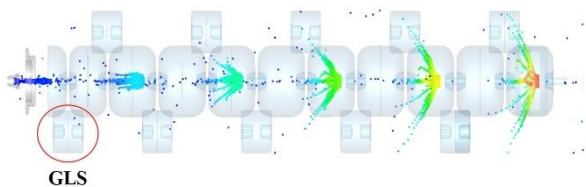


Figure 7: Beam dynamics simulation when GLS is 0.8.

Table 1: Optimized Parameters for three GLSs

GLS	Current (A)	Energy (MeV)
0.8	0.85	9.98
0.9	0.82	9.91
1.0	0.75	9.80

## PARAMETERS OF OPTIMIZED LINAC STRUCTURE

After performing numerous CST simulations (CST MICROWAVE STUDIO) using the eigenmode solver and frequency domain solver, the geometries of the normal accelerating cells, the bunching cells, and the power coupler cell were optimized. As shown in the Fig. 8, the electric field distribution of the structure was optimized at 2853 MHz for the  $\pi/2$  operation mode. Its best optimized RF parameters are summarized in Table 2 [12]. To obtain a higher shunt impedance, the geometry of the nose-cone was optimized. Optimized RF parameters are close to our target ones as summarized in Table 2. Among three GLSs, distribution of electric field is best when GLS is 0.8 as shown in Figs. 7 and 8.

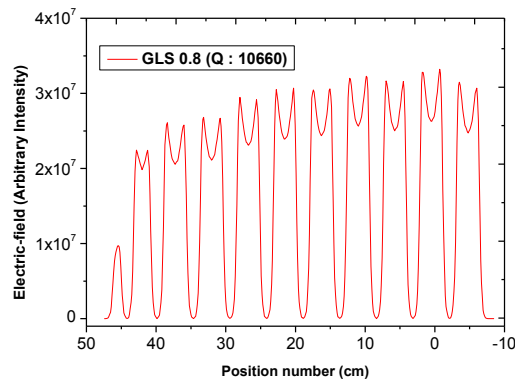


Figure 8: Electric field optimization result when GLS is 0.8.

Table 2: RF Parameters of Optimized Linac Structure

RF Property	Value	Unit
Frequency	2853	MHz
Length of linac	0.57	m
Quality factor $Q_0$	10660	.
Standing Wave Ratio (SWR)	1.3	.
Shunt impedance, $R_{sh}$	70	M $\Omega$ /m
Average external coupling	3.06	.
Operation mode	$\pi/2$	.
Beam current	50	mA
Input power for 9 MeV	3	MW
Input power for 6 MeV	1.5	MW

## SUMMARY

A shunt impedance of 70 M $\Omega$ /m and a quality factor of 10660 at the  $\pi/2$  mode frequency of 2853 MHz were obtained with an average external coupling coefficient of 3.06 and a standing wave ratio of 1.3. The RF parameters and a drawing of the S-band linac structure were devised via a CST simulation and subsequently, the linac structure was fabricated. Finally, the best result for the Q-factor and electric field flatness was obtained when the diameter of the bunching cells is 75.8 mm and that of the power coupler cell is 75.2 mm. We realized that the ratio of electric field between bunching cells and normal accelerating cells can be adjusted by tuning gap between side-coupling cells. Now, we are trying to improve uniformity of electric field along the structure further.

## REFERENCES

- [1] P. K. Ambattu *et al.*, "Low energy RF accelerator for various applications.", in *Proc. Linac'10*, Tsukuba, Japan, paper, M-OP033, p. 127.
- [2] American National Standard for Determination of the Imaging Performance of X-Ray and Gamma-Ray Systems for Cargo and Vehicle Security Screening, 2008, N42.46-2008.

- Content from this work may be used under the terms of the CC BY 3.0 licence (© 2018). Any distribution of this work must maintain attribution to the author(s), title of the work, publisher, and DOI.
- [3] Aleksandr Y. Saverskiy *et al.*, “Cargo and Container X-Ray Inspection with Intra-Pulse Multi-Energy Method for Material Discrimination”, in *Proc. CAARI 2014*, **66**, pp. 232-241, 2015.
- [4] P. Buaphad *et al.*, “6/9 MeV S-band Standing Wave Accelerating Structure for Container X-ray Inspection System at RTX” in *Proc. IPAC’16*, Busan, Korea, May 2016, paper TUPOY010, pp. 1924-1926.
- [5] Y. Kim, Lecture Note on Advanced Beam Dynamics for XFEL Projects, 2011.
- [6] H. Yang *et al.*, “Transverse RF focusing in bunching cells for standing-wave LINAC”, *Nuclear Instruments and Methods in Physics A*, **703**, pp. 145–151, 2013.
- [7] H. Miller *et al.*, “Comparison of Standing-wave and Traveling-wave Structures” in *Proc. Linac’86*, Stanford, California, paper TU2-4.
- [8] Y. Li *et al.*, Technique Report on “Simulation and Design of RF LINAC.”, internal technical report.
- [9] S. Ahmadiannamin *et al.*, “Design and Simulation of Side Coupled six MeV LINAC for X-ray Cargo Inspection”, in *Proc. IPAC’14*, Dresden, Germany, Jun 2014, paper THPRI035, pp. 3844-3846.
- [10] D. Alesini *et al.*, “Power coupling”, arXiv:1112.3201, LNF, INFN, Frascati, Italy, CERN Yellow Report CERN-2011-007, pp. 125-147, 2011.
- [11] N. Nepal, *et al.*, “Design Study on Standing-Wave Linear Accelerator”, in *Proc. IPAC2001*, Chicago, IL Jun 18-22, 2001, paper WPPH317, p. 2802.
- [12] P. Schmuser *et al.*, “Tuning of Multi-Cell Cavities Using Bead Pull Measurements”, SRF920925-10, Cornell University Internal Report, 1992.